Identification of new transitions and levels in ^{163}Gd from β-decay studies

C. J. Zachary,[1,*] N. T. Brewer,[1,2] J. C. Batchelder,[3] E. Wang,[1] J. H. Hamilton,[1] J. M. Eldridge,[1] B. M. Musangu,[1] A. V. Ramayya,[1] C. J. Gross,[2] K. P. Rykaczewski,[2] R. Grzywacz,[4,2] A. C. Dai,[5] F. R. Xu,[5] Y. X. Liu,[6] Y. Sun,[7] M. Madurga,[4] D. Miller,[4] D. W. Stracener,[2] C. Jost,[4] E. F. Zganjar,[8] J. A. Winger,[9] M. Karny,[2] S. V. Paulauskas,[4] S. H. Liu,[10] M. Wolińska-Cichocka,[2,11] S. W. Padgett,[4] A. J. Mendez,[12] K. Miernik,[2,13] A. Fijałkowska,[4,13] and S. V. Ilyushkin[9]

[1]*Department of Physics and Astronomy, Vanderbilt University Nashville, Tennessee 37240, USA*
[2]*Physics Division, Oak Ridge National Laboratory, Oak Ridge, Tennessee 37931, USA*
[3]*Nuclear Engineering Department, University of California Berkeley, California 94720, USA*
[4]*Department of Physics and Astronomy, University of Tennessee, Knoxville, Tennessee 37996, USA*
[5]*School of Physics, Peking University, Beijing 100871, People's Republic of China*
[6]*School of Science, Huzhou University, Huzhou 313000, People's Republic of China*
[7]*School of Physics and Astronomy, Shanghai Jiao Tong University, Shanghai 200240, People's Republic of China*
[8]*Department of Physics and Astronomy, Louisiana State University, Baton Rouge, Louisiana 70803, USA*
[9]*Department of Physics and Astronomy, Mississippi State University, Mississippi 39762, USA*
[10]*UNIRIB/Oak Ridge Associated Universities, Oak Ridge, Tennessee 37831, USA*
[11]*Heavy Ion Laboratory, University of Warsaw, Warsaw, PL 02-093, Poland*
[12]*Campbell University, Buies Creek, North Carolina 27506, USA*
[13]*Faculty of Physics, University of Warsaw, Warsaw, PL 02-093, Poland*

(Received 18 February 2020; revised manuscript received 7 April 2020; accepted 27 April 2020; published 19 May 2020)

Background: Neutron-rich nuclei in the mass region around $A = 160$ have been and will continue to be of interest for the study of nuclear structure because of the rapid onset of deformation between 88 and 90 neutrons. The observation of detailed changes in nuclear structures within this mass region has provided and will continue to provide insight into the nuclear force.
Purpose: Investigations of γ rays emitted following ^{163}Eu β-decay to ^{163}Gd have been performed for evaluation of the nuclear structure of ^{163}Gd.
Method: Data were collected at the LeRIBSS station of the Holifield Radioactive Ion Beam Facility at Oak Ridge National Laboratory with an array of four Clover HPGe detectors for γ-rays and two plastic scintillators for β detection. The γ rays were identified as belonging to ^{163}Gd via mass selection and γ-γ-β, x-ray-γ, or γ-γ coincidences.
Results: In total 107 new γ-ray transitions were observed in ^{163}Gd from 53 newly identified levels.
Conclusions: The structure of ^{163}Gd has been identified for the first time. This structure has been evaluated in comparison to projected shell model, and potential energy surface calculations with good agreement.

DOI: 10.1103/PhysRevC.101.054312

I. INTRODUCTION

The rapid onset of deformation between 88 and 90 neutrons has triggered nuclear structure studies with the aim of revealing the origin and extent of this phenomenon. Observations by Jones *et al.* [1] documented an interruption in the continuous drop in first 2^+ energy with increasing neutron number between $N = 98$ ^{162}Gd and $N = 100$ ^{164}Gd. This observation was in contrast to expectations that 2^+ energy would decrease smoothly to a lowest 2^+ energy and largest deformation at midshell $N = 104$ [1]. A subshell gap at $N = 98$ is discussed by Hartley *et al.* [2] as explanation for this aberration in the 2^+ energies. Study of $N = 99$ ^{163}Gd can provide new insights into neutron single-particle orbitals in $N = 99$ nuclei to better understand this region. Investigations following β decay in the mass region around $A = 160$ aided by potential energy surface and shell-model calculations are helpful to the analysis of the effects of the nuclear force governing nuclear shapes and the resulting sequence of single-particle orbitals. This work on ^{163}Gd is the result of one such investigation from europium 162–165 isotopes, which were produced at the Holifield Radioactive Ion Beam Facility in Oak Ridge National Laboratory for β-decay studies of levels in the daughter isotopes of gadolinium 162–165.

Previous total absorption studies by Hayashi *et al.* [3] have identified the Q_β for ^{163}Gd as 3170(70) keV. A Q_β for ^{163}Eu of 4918(6) was obtained from Vilen *et al.*'s precision mass measurements using JYFLTRAP [4]. A study with the JAEA-ISOL by Sato *et al.* [5] identified five transitions with energies

*christopher.j.zachary@vanderbilt.edu

85.8, 116, 138, 191.2, and 401 keV in ^{163}Gd without level assignments. In the present work, all of the five previously observed transitions have been confirmed and 107 new transitions identified, 22 of which are tentative, between 53 new levels, three of which are tentative. The configurations of newly identified rotational band structures of ^{163}Gd are based upon systematics for $N = 99$ low-energy rotational band structure of ^{165}Dy [6–8] and projected shell-model calculations, which support the assigned level structure. In addition many new high-energy levels have been observed for ^{163}Gd.

An isomer has been observed previously in ^{163}Gd by Hayashi *et al.* with a half-life of 23.5(10)s [3]. This is of special interest in the low-energy band structure of ^{163}Gd. Consistent with Hayashi *et al.*'s [3] observation, this work assigns the ground state as the $7/2^+[633]$ with the $1/2^-[521]$ being the low-energy isomeric state observed by Hayashi *et al.* [3]. Such an assignment would result in an isomeric transition between the $1/2^-[521]$ and $7/2^+[633]$ levels. Projected shell-model calculations included in this work confirm this relationship with good agreement between proposed levels and calculated excitations.

The elevation of the $1/2^-[521]$ above the $7/2^+[633]$ for $N = 99$ provide further evidence for the subshell gap beginning at $N = 98$, as discussed in the study of nearby mass ^{162}Gd by Hartley *et al.* [2], a description further supported by the observed excitation energy of the $5/2^-[523]$ 1-qp state.

II. EXPERIMENTAL METHODS

For this study a 10–18 μA beam of 50 MeV protons was used to induce fission in a UCx target on a high-voltage platform to produce $^{162–165}$Eu via fission at the Holifield Radioactive Ion Beam Facility at Oak Ridge National Laboratory. After fission, ions were accelerated off the HV platform and passed through a high-resolution isobar separator that provided an isotopically pure beam to LeRIBSS. The beam was implanted onto a movable tape. After a designated measurement time, the moving tape controller (MTC) would transport the accumulated source behind a shield to prevent additional background from undesired daughter products, then a new source would be collected. This is referred to here as the tape cycle. The MTC settings for source collection time and measurement time were selected to best allow for observation of wanted products as selected from previously measured half-lives of europium and gadolinium isotopes. These settings were for a 30 s collection time and a 25 s decay time. For ^{163}Eu the half-life was measured by Osa *et al.* [9] to be 7.7(4)s, by Sato *et al.* [5] to be 7.8(5)s, and by Wu *et al.* [10] to be 8.1(16)s. The half-life of ^{163}Gd was measured as 68(3)s by Gehrke *et al.* [11].

The detector array used was a Clover Array for Radioactive Decay Spectroscopy (CARDS) of four HPGe clover detectors, for the detection of γ rays, operated without Compton suppression, oriented around the beam line. The four Clover detectors were located on a single plane normal to the beam line with 90° angles between each adjacent Clover. Adjacent the HPGe clovers were two plastic scintillators for β-ray detection. The scintillators allowed for gating on β signals with coincident γ-ray signals without obtaining β spectroscopy. Data acquisition was via digital pulse processing with Pixie16 modules according to methods detailed by Grzywacz [12]. This array allowed for coincident analysis with γ-γ, x-ray-γ, γ-tape cycle, γ-β-tape cycle, and associated projections.

III. RESULTS

The five previously identified transitions have been observed in this work to be 85.3, 116.1, 138.2, 191.7, and (401.6) keV. These previously identified transitions and the characteristic x rays for ^{163}Gd were used to confirm transitions associated with the deexcitation of ^{163}Gd via $\gamma - \gamma$, x-ray-γ, $\beta - \gamma$, and γ-tape-cycle coincidences. Additionally 107 new transitions have been identified, 22 of which are tentative, between 53 new levels, 3 of which are tentative. The full decay scheme obtained in this work is shown in Figs. 1 and 2.

Figures 3(j) and 3(k) show spectra of those γ transitions coincident with the 85.3 keV transition. Therein are clearly observed the 104.6, 441.2, 446.7, (487.4), (952.1), 975.8, 992.9, 1015.4, 1428.5, and 1713.0 keV transitions. Gates on each of these transitions are consistent with their assignments. The gate on the 104.6 keV γ ray, not shown, allows observation of the 651.3 keV transition, which is of low intensity and is not distinguishable from the background in the coincidence spectra of the strong 85.3 keV transition. Also seen in the 85.3 keV coincidence spectra are evidences for a number of transitions that are not observed in gates for any other transitions but whose coincidence spectra are consistent with their assignment: 607.9, 672.2, 2178.6, 2235.6, 2246.8, 2310.8, (2431.2), (2490.9), and (2577.3) keV transitions. Furthermore the 2319.2 and 2326.3 keV transitions are contributing to this spectra though not well resolved from the 2310.8 keV peak in this frame.

Seen in Figs. 3(h) and 3(i) are transitions coincident with the 191.7 keV transition; (52.8), 72.2, 74.6, 96.8, (130.6), 171.1, 1002.0, (1834.9), 1858.7, 1910.5, 2030.4, and 2126.6 keV. The (52.8) keV transition in this gate is weakly observed on the shoulder of the 50 keV x-ray peak and would correspond to feeding from the 454.5 keV level. However, the (52.8) keV transition is in a region of very strong internal conversion and gates upon the (52.8) keV transition do not confirm this assignment, therefore, it is only tentatively placed. The (130.6) keV transition matches the energy to originate from the 532.1 keV level to the 401.7 keV level, but a gate on (130.6) keV does not show all of the expected coincident transitions and is thus included tentatively.

In Fig. 3(f) are seen transitions coincident with the 1758.2 keV transition. The 400.4, 516.7, and 538.8 keV transitions demonstrate clear coincidence with the 1758.2 keV transition. Similarly, Fig. 3(d) shows coincident spectra for the gate on the 1815.9 keV transition. The transitions of 459.1, 481.3, and 531.0 keV are observed without clear observation of any additional transitions.

In Fig. 3(g) are seen the coincidence spectra for a gate on the 1037.1 keV transition, demonstrating coincidence with the 1226.1, 1359.9, 1402.8, 1447.8, and 1491.1 keV transitions. In Fig. 3(e) are seen the coincidence spectra for a gate on the 454.5 keV transition, demonstrating coincidence with the

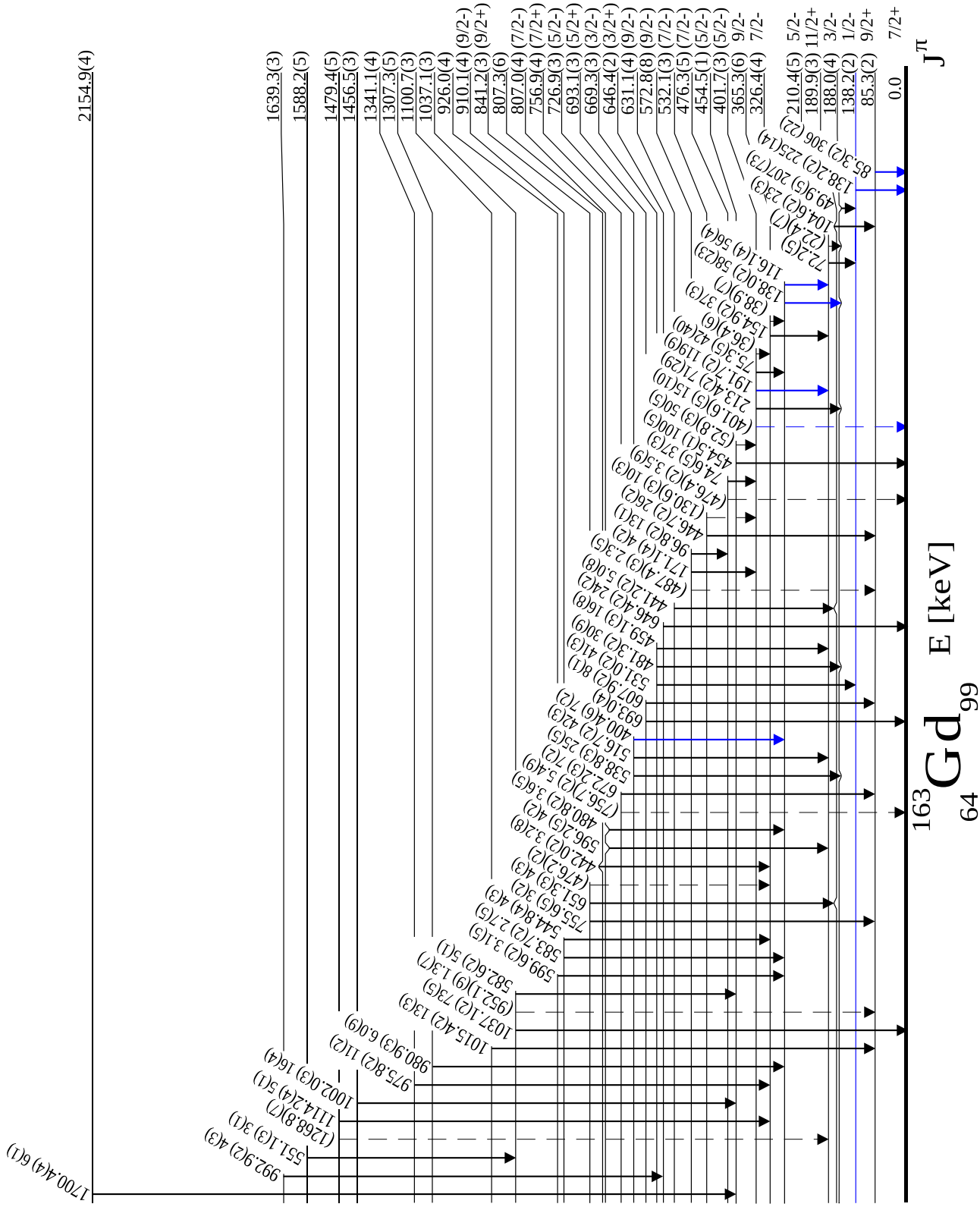

FIG. 1. Level scheme of ^{163}Gd. New transitions and levels in black, previously identified transitions and the isomeric level in blue. $T_{1/2}$ of the 138.2 keV level is 23.5(10)s[3]. Tentative transitions are indicated by dashed arrow and parentheses around transition energy. Listed intensity values are corrected for internal conversion.

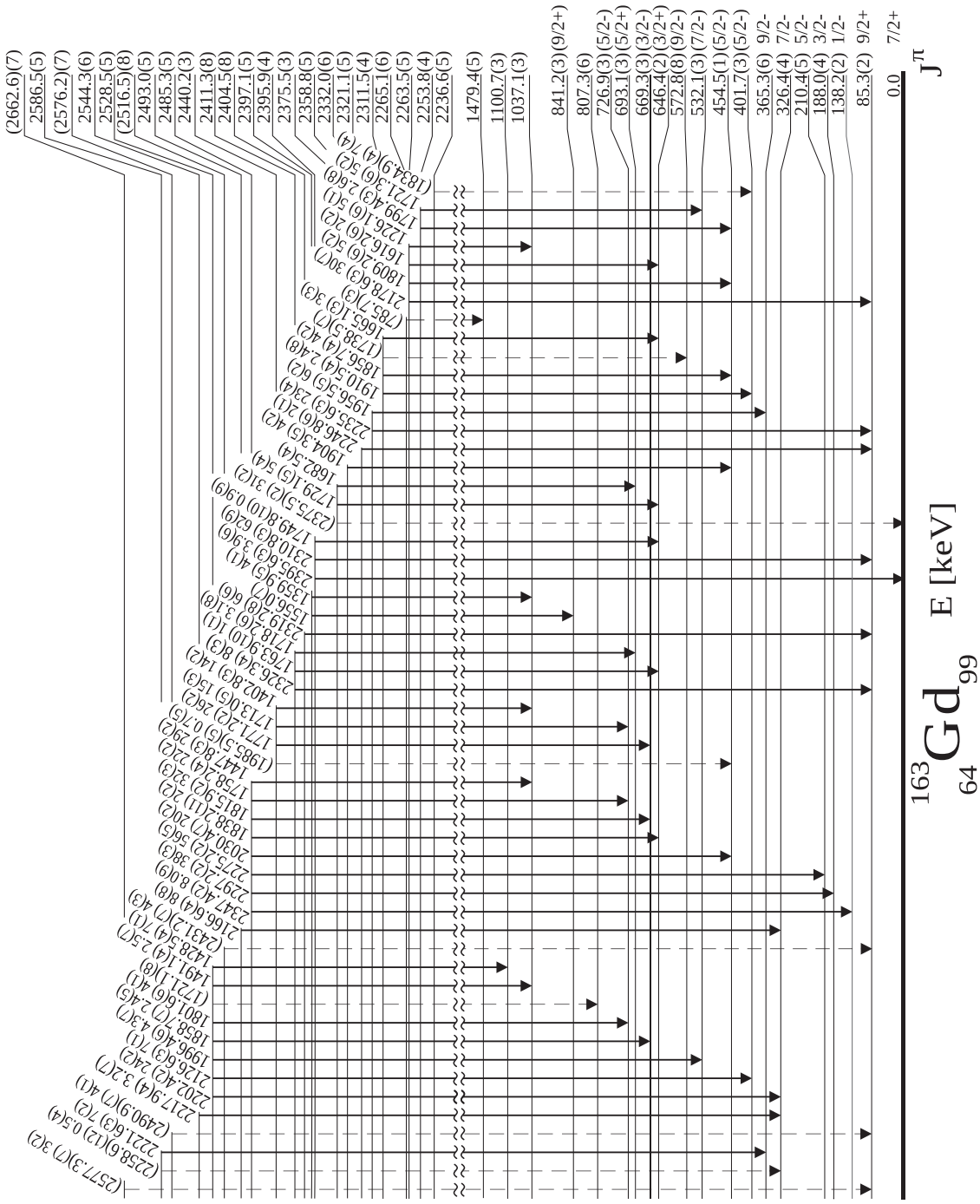

FIG. 2. Level scheme of ^{163}Gd continued. New transitions and levels in black, previously identified isomeric level in blue. Tentative levels indicated with parentheses around level energy. Tentative transitions are indicated by dashed arrow and parentheses around transition energy.

1002.0, 1700.4, 1799.4, 1809.2, 1856.7, 1904.3, (1985.5), and 2030.4 keV transitions.

Figures 3(a) and 3(b) are gates upon the 138.0 and 116.1 keV transitions, respectively. Evidence is seen in these separate gates for the 72.2 keV transition and the 49.9 keV transition, respectively. Note that while the 49.9 keV peak appears in both spectra, it is strongly enhanced in the 138.0 keV gate because this transition overlaps in energy the K_b x rays for ^{163}Gd. The enhancement observed only in the 138.0 keV gate is because the 49.9 keV coincident γ-ray transition adds intensity to the x-ray peak while the peak observed in 116.1 keV gate is expected to be predominantly from the K_b x rays from ^{163}Gd. Observed between both gates are also the 75.3, 400.4, 480.8, 583.7, and 599.6 keV transitions. The higher-energy 2166.6, 2202.4, 2217.9, and (2258.6) keV transitions, which feed the 326.4 keV level from higher in the structure are shown in Fig. 3(a) and are also observed in the gate upon 116.1 keV though not shown here.

Figure 3(c) displays the spectra obtained from a gate on 646.4 keV. Here is observed evidences for the 992.9, 1616.2,

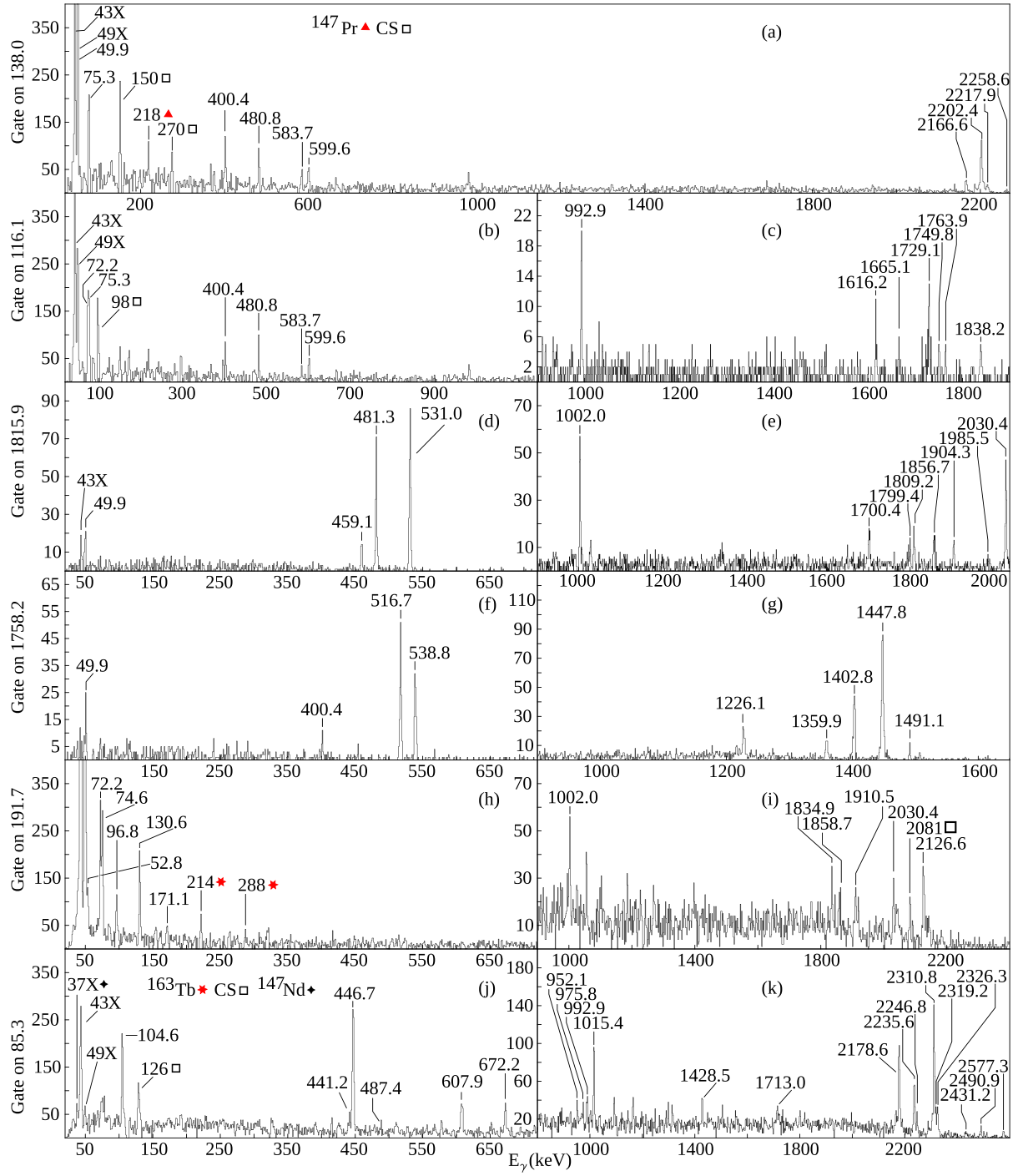

FIG. 3. Coincidence spectra for background subtracted gates on ^{163}Gd transitions; (a) 138.0 keV, (b) 116.1 keV, (c) 646.4 keV, (d) 1815.9 keV, (e) 454.5 keV, (f) 1758.2 keV, (g) 1037.1 keV, (h), (i) 191.7 keV, (j), (k) 85.3 keV. Where CS indicates a Compton scatter peak and peaks from x rays are marked with an X.

1665.1, 1729.1, 1749.8, 1763.9, and 1838.2 keV transitions to the 646.4 keV level. The 646.4 keV level is tentatively assigned as the $3/2^+$ band head, along with rotational excitations at levels 693.1, 756.9, and 841.2 keV as discussed in the following section.

As for the remaining transitions identified in ^{163}Gd at 2347.4, (2375.5), and 2395.6 keV, they are not clearly present in the coincidence gates shown but are coincident with appropriate K x-ray peaks, and are present in the singles spectra, not shown. The (2375.5) keV transition is listed as tentative due to a lack of any other observed transitions coincident with the (2375.5) keV transition, an alternate location for this transition would be feeding the 138.2 keV $1/2^-$ level, which is an isomer and feeding to this state would be consistent with no observation of other coincident transitions.

TABLE I. Transitions in ^{163}Gd. Transition energy with tentative assignments in parentheses, relative intensity, internal conversion corrected relative intensity obtained using coefficients from *BrIcc* [13], assumed multipolarity for ICC, energy and J^π of initial and final levels. J^π assignments from systematics with ^{165}Dy [6–8]. Uncertainties listed account only for uncertainty of the γ-ray observations.

E_γ keV	I_γ	I_{total}	ICC & Multipolarity	E_i	E_f	J_i^π	J_f^π
(22.4)(7)				210.4(5)	188.0(4)	$5/2^-$	$3/2^-$
(36.4)(6)				401.7(3)	365.3(6)	$(5/2^-)$	$9/2^-$
38.9(7)				365.3(6)	326.4(4)	$9/2^-$	$7/2^-$
49.9(5)	61(22)	207(73)	2.37 $M1$	188.0(4)	138.2(2)	$3/2^-$	$1/2^-$
(52.8)(3)	3.6(4)	50(5)	12.66 $M1$	454.5(1)	401.7(3)	$(5/2^-)$	$(5/2^-)$
72.2(5)				210.4(5)	138.2(2)	$5/2^-$	$1/2^-$
74.6(5)	6.5(5)	37(3)	4.68 $M1$	476.3(5)	401.7(3)	$(7/2^-)$	$(5/2^-)$
75.3(5)	8(7)	42(40)	4.56 $M1$	401.7(3)	326.4(4)	$(5/2^-)$	$7/2^-$
85.3(2)	73(5)	306(22)	3.18 $M1$	85.3(2)	0.0	$9/2^+$	$7/2^+$
96.8(2)	4.0(3)	13(1)	2.21 $M1$	572.8(8)	476.3(5)	$(9/2^-)$	$(7/2^-)$
104.6(2)	8(1)	23(3)	1.77 $M1$	189.9(3)	85.3(2)	$11/2^+$	$9/2^+$
116.1(4)	24(2)	56(4)	1.31 $M1$	326.4(4)	210.4(5)	$7/2^-$	$5/2^-$
(130.6)(3)	5(1)	10(3)	0.94 $M1$	532.1(3)	401.7(3)	$(7/2^-)$	$(5/2^-)$
138.0(2)	32(13)	58(23)	0.79 $E2$	326.4(4)	188.0(4)	$7/2^-$	$3/2^-$
138.2(2)	26(2)	225(14)	7.66 $E3$	138.2(2)	0.0	$1/2^-$	$7/2^+$
154.9(2)	24(2)	37(3)	0.53 $E2$	365.3(6)	210.4(5)	$9/2^-$	$5/2^-$
171.1(4)	3(1)	4(2)	0.38 $E2$	572.8(8)	401.7(3)	$(9/2^-)$	$(5/2^-)$
191.7(2)	90(6)	119(9)	0.32 $M1$	401.7(3)	210.4(5)	$(5/2^-)$	$5/2^-$
213.4(2)	57(23)	71(29)	0.24 $M1$	401.7(3)	188.0(4)	$(5/2^-)$	$3/2^-$

Tables I, II, and III list every transition observed in ^{163}Gd. The relative intensities are referenced to the 454.5 keV transition with uncertainties of the last digit indicated in parentheses. The internal conversion corrected intensities obtained with coefficients from *BrIcc* [13] and the multipolarities assumed for these corrections are shown in Table I, the uncertainties shown are only the uncertainty in the observation of the γ ray and do not account for possible multipolarity mixing. The energy of the initial and final levels as well as the spins of the initial and final levels for those levels with spin assignments are also shown.

IV. DISCUSSION

The level schemes in Figs. 1 and 2 have been assembled based upon observed coincidences, intensity, and assigned level spacings. Choice of the ground state was informed by the structure of ^{165}Dy [7,8] and confirmed by subsequent identification of transitions to the ground state. All spin assignments have been based upon systematics with ^{165}Dy [7,8] and are supported by theoretical calculations discussed below.

The previously observed 85.3, 138.0, and (401.6) keV transitions and the newly observed 454.5, (476.4), 1037.1, (2375.5), 2395.6 keV transitions have been placed as populating the ground state, which has been assigned a spin value of $7/2^+$. This assignment of $7/2^+$ as the ground state of ^{163}Gd is based upon systematics with ^{165}Dy [6–8]. Assignment of the $1/2^-$ band in ^{163}Gd was based upon systematics of the $1/2^-$ band structure observed in ^{165}Dy. A very similar structure is observed for the $1/2^-$ band in ^{165}Dy and in ^{163}Gd. In ^{165}Dy the following transitions are observed within the first $1/2^-$ band: 50.4, 72.8, 116.8, 139.1, and 156.2 for which the analogs in the proposed $1/2^-$ band in ^{163}Gd are 49.9, 72.2, 116.1, 138.0, and 154.9 keV. These transitions have been listed according to the levels between which they are observed in ^{165}Dy and the matching spin levels where they are proposed to be transitions in ^{163}Gd. Additional lower-energy transitions within the first $1/2^-$ band of ^{165}Dy were observed at the energies of 22.4 and 39.5 keV, and according to the proposed scheme, would be expected within ^{163}Gd to be 22.4 and 38.9 keV. However, these transitions are in an energy region for which the internal conversion is very strong, there is significant contamination from x rays, and the efficiency of the Clover detectors is dropping rapidly in the region of the 22.4 keV transition. Thus, there not being direct observation of the 22.4 keV transition within the scope of this study is not disconcerting and has been included tentatively in the proposed level scheme based upon observations of subsequent transitions in gates, which would otherwise not be coincident.

The 138.2 keV transition to ground has no clear direct observation in this work due to the presence of a transition of nearly degenerate energy 138.0 keV. However, this transition exhibits enhancement of intensity in the singles spectrum consistent with the previously observed isomeric transition of 137.8 keV by Hayashi *et al.* [3]. With the observed peak intensity enhancement and the matching spacing of the associated single-particle state, the $1/2^-$ band head is assigned to have an excitation of 138.2 keV. If it is taken that both the 108.2 keV transition in ^{165}Dy and the 138.2 keV transition in ^{163}Gd are pure $E3$ transitions, the half-life of the 138.2 keV transition can be roughly estimated according to the reduced transition probabilities for $E3$ transitions by assuming the same reduced transition probability for both transitions. As the half-life of the 108.2 keV transition was observed to be 1.257 min [14], the half-life of the 138.2 keV transition would be estimated as 13.6 s. This is according to the energy relationship for reduced transition probabilities as discussed in Alder and Steffen's text [15]. Hayashi *et al.*'s observation of a 23.5(10)s

TABLE II. Transitions in ^{163}Gd (cont.).

E_γ keV	I_γ	E_i	E_f	J_i^π	J_f^π
400.4(6)	7(2)	726.9(3)	326.4(4)	$(5/2^-)$	$7/2^-$
(401.6)(5)	15(10)	401.7(3)	0.0	$(5/2^-)$	$7/2^+$
441.2(2)	5.0(8)	631.1(4)	189.9(3)	$(9/2^-)$	$11/2^+$
442.0(2)	3.2(8)	807.3(6)	365.3(6)		$9/2^-$
446.7(2)	26(2)	532.1(3)	85.3(2)	$(7/2^-)$	$9/2^+$
454.5(1)	100(5)	454.5(1)	0.0	$(5/2^-)$	$7/2^+$
459.1(3)	16(8)	669.3(3)	210.4(5)	$(3/2^-)$	$5/2^-$
(476.2)(2)		841.2(3)	365.3(6)	$(7/2^-)$	$9/2^-$
(476.4)(2)	3.5(9)	476.3(5)	0.0	$(9/2^+)$	$7/2^+$
480.8(2)	3.6(5)	807.0(4)	326.4(4)	$(7/2^-)$	$7/2^-$
481.3(2)	30(9)	669.3(3)	188.0(4)	$(3/2^-)$	$3/2^-$
(487.4)(3)	2.3(5)	572.8(8)	85.3(2)	$(9/2^-)$	$9/2^+$
516.7(2)	42(3)	726.9(3)	210.4(5)	$(5/2^-)$	$5/2^-$
531.0(2)	41(3)	669.3(3)	138.2(2)	$(3/2^-)$	$1/2^-$
538.8(3)	25(5)	726.9(3)	188.0(4)	$(5/2^-)$	$3/2^-$
544.8(4)	4(3)	910.1(4)	365.3(6)	$(9/2^-)$	$9/2^-$
551.1(3)	3(1)	1588.2(5)	1037.1(3)		
582.6(2)	5(1)	1037.1(3)	454.5(1)		$(5/2^-)$
583.7(2)	2.7(5)	910.1(4)	326.4(4)	$(9/2^-)$	$7/2^-$
596.2(5)	4(2)	807.0(4)	210.4(5)	$(7/2^-)$	$5/2^-$
599.6(2)	3.1(5)	926.0(4)	326.4(4)		$7/2^-$
607.9(2)	8(1)	693.1(3)	85.3(2)	$(5/2^+)$	$9/2^+$
646.4(2)	24(2)	646.4(2)	0.0	$(3/2^+)$	$7/2^+$
651.3(3)	4(3)	841.2(3)	189.9(3)	$(9/2^+)$	$11/2^+$
672.2(3)	7(2)	756.9(4)	85.3(2)	$(7/2^+)$	$9/2^+$
693.0(4)		693.1(3)	0.0	$(5/2^+)$	$7/2^+$
755.6(5)	3(2)	841.2(3)	85.3(2)	$(9/2^+)$	$9/2^+$
(756.7)(2)	5.4(9)	756.9(4)	0.0	$(7/2^+)$	$7/2^+$
(785.7)(3)		2265.1(6)	1479.4(5)		
(952.1)(9)	1.3(7)	1037.1(3)	85.3(2)		$9/2^+$
975.8(2)	11(2)	1341.1(4)	365.3(6)		$9/2^-$
980.9(3)	6.0(9)	1307.3(5)	326.4(4)		$7/2^-$
992.9(2)	4(3)	1639.3(3)	646.4(2)		$(3/2^+)$
1002.0(3)	16(4)	1456.5(3)	454.5(1)		$(5/2^-)$
1015.4(2)	13(3)	1100.7(3)	85.3(2)		$9/2^+$
1037.1(2)	73(5)	1037.1(3)	0.0		$7/2^+$
1114.2(4)	5(1)	1479.4(5)	365.3(6)		$9/2^-$
1226.1(6)	5(1)	2263.5(5)	1037.1(3)		
(1268.8)(7)		1479.4(5)	210.4(5)		$5/2^-$
1359.9(5)	4(1)	2397.1(5)	1037.1(3)		
1402.8(3)	14(2)	2440.2(3)	1037.1(3)		
1428.5(4)	7(1)	2528.5(5)	1100.7(3)		
1447.8(3)	29(2)	2485.3(5)	1037.1(3)		
1491.1(4)	2.5(7)	2528.5(5)	1037.1(3)		
1556.0(7)		2397.1(5)	841.2(3)		$(9/2^+)$
1616.2(6)	2(2)	2263.5(5)	646.4(2)		$(3/2^+)$
1665.1(3)	3(3)	2311.5(4)	646.4(2)		$(3/2^+)$
1682.5(4)		2375.5(3)	693.1(3)		$(5/2^+)$
1700.4(4)	6(1)	2154.9(4)	454.5(1)		$(5/2^-)$
1713.0(5)	15(3)	2440.2(3)	726.9(3)		$(5/2^-)$
1718.2(6)	3.1(8)	2411.3(8)	693.1(3)		$(5/2^+)$
(1721.1)(8)		2528.5(6)	807.3(6)		$(7/2^-)$

TABLE III. Transitions in ^{163}Gd (cont.).

E_γ keV	I_γ	E_i	E_f	J_i^π	J_f^π
1721.3(6)	5(2)	2253.8(4)	532.1(3)		$(7/2^-)$
1729.1(5)	5(4)	2375.5(3)	646.4(2)		$(3/2^+)$
(1738.5)(7)		2311.5(4)	572.8(8)		$(9/2^-)$
1749.8(10)	0.9(9)	2395.9(4)	646.4(2)		$(3/2^+)$
1758.2(4)	22(2)	2485.3(5)	726.9(3)		$(5/2^-)$
1763.9(10)	1(1)	2411.3(8)	646.4(2)		$(3/2^+)$
1771.2(2)	26(2)	2440.2(3)	669.3(3)		$(3/2^-)$
1799.4(3)	2.6(8)	2253.8(4)	454.5(1)		$(5/2^-)$
1801.6(6)	4(1)	2528.5(5)	726.9(3)		$(5/2^-)$
1809.2(6)	5(2)	2263.5(5)	454.5(1)		$(5/2^-)$
1815.9(2)	32(3)	2485.3(5)	669.3(3)		$(3/2^-)$
(1834.9)(4)	7(4)	2236.6(5)	401.7(3)		$(5/2^-)$
1838.2(11)	2(2)	2485.3(5)	646.4(2)		$(3/2^+)$
1856.7(4)	4(2)	2311.5(4)	454.5(1)		$(5/2^-)$
1858.7(7)	2.4(5)	2528.5(5)	669.3(3)		$(3/2^-)$
1904.3(5)	4(2)	2358.8(5)	454.5(1)		$(5/2^-)$
1910.5(4)	2.4(8)	2311.5(4)	401.7(3)		$(5/2^-)$
1956.5(5)	6(2)	2321.1(5)	365.3(6)		$9/2^-$
(1985.5)(5)	0.7(5)	2440.2(3)	454.5(1)		$(5/2^-)$
1996.4(6)	4.3(7)	2528.5(5)	532.1(3)		$(7/2^-)$
2030.4(7)	20(2)	2485.3(5)	454.5(1)		$(5/2^-)$
2126.6(3)	7(1)	2528.5(5)	401.7(3)		$(5/2^-)$
2166.6(4)	8(8)	2493.0(5)	326.4(4)		$7/2^-$
2178.6(3)	30(7)	2263.5(5)	85.3(2)		$9/2^+$
2202.4(2)	24(2)	2528.5(5)	326.4(4)		$7/2^-$
2217.9(4)	3.2(7)	2544.3(6)	326.4(4)		$7/2^-$
2221.6(3)	7(2)	2586.5(5)	365.3(6)		$9/2^-$
2235.6(3)	23(4)	2321.1(5)	85.3(2)		$9/2^+$
2246.8(6)	2(1)	2332.0(6)	85.3(2)		$9/2^+$
(2258.6)(12)	0.5(4)	2586.5(5)	326.4(4)		$7/2^-$
2275.2(2)	56(5)	2485.3(5)	210.4(5)		$5/2^-$
2297.2(2)	38(3)	2485.3(5)	188.0(4)		$3/2^-$
2310.8(3)	62(9)	2395.9(4)	85.3(2)		$9/2^+$
2319.2(8)	6(6)	2404.5(8)	85.3(2)		$9/2^+$
2326.3(4)	8(3)	2411.3(8)	85.3(2)		$9/2^+$
2347.4(2)	8.0(9)	2485.3(5)	138.2(2)		$1/2^-$
(2375.5)(2)	31(2)	2375.5(3)	0.0		$7/2^+$
2395.6(3)	3.9(6)	2395.9(4)	0.0		$7/2^+$
(2431.2)(7)	4(3)	2516.5(8)	85.3(2)		$9/2^+$
(2490.9)(7)	4(1)	2576.2(7)	85.3(2)		$9/2^+$
(2577.3)(7)	3(2)	2662.6(7)	85.3(2)		$9/2^+$

half-life is then consistent with an $E3$ transition [3]. As there is only a single γ transition following the proposed isomer, a half-life on the order of seconds would prevent the experimental setup from observing any coincident γ rays or β rays. This would result in enhancement of the transition in the singles spectrum without any further evidence and an observed excess of γ feeding compared to γ outflow for the associated level. which is consistent with our observations. Furthermore the assignment of $1/2^-$ being above the $7/2^+$ state is consistent with studies by Hartley, *et al.* [2]. Wherein the ordering of the $\nu 7/2[633]$, $\nu 1/2[521]$, and $\nu 5/2[523]$ single-particle states is well discussed for the nearby $N = 98$ ^{162}Gd.

Assignment of the $3/2^-$ band comes from the six strongest transitions observed exiting the band in Figs. 3(d) and 3(f). The gate on 1758.2 keV shown in Fig. 3(f) shows the 400.4, 516.7, and 538.8 keV transitions, which correspond to the three transitions from the 726.9 keV $(5/2^-)$ level to the 326.4 keV $7/2^-$, 210.4 keV $5/2^-$, and 188.0 keV $3/2^-$ levels,

TABLE IV. Internal conversion corrected γ feeding and γ outflow in ^{163}Gd. J^π assignments in the current work from systematics with ^{165}Dy [6–8]. [‡]Expected isomeric state. [†]Neither the expected 22.4 keV transition from 210.4 keV level to 188.0 keV level nor the 72.2 keV transition to the 138.2 keV level could be fit for relative intensity assignment.

E_{Level} keV	γ Feeding	γ Outflow	J^π	E_{Level} keV	γ Feeding	γ Outflow	J^π
0.0[a]	787(30)		$7/2^+$	1456.5(3)		16(4)	
85.3(2)	225(15)	306(22)	$9/2^+$	1479.4(5)[a,b]		5(1)	
138.2(2)[‡a]	256(73)	224(14)	$1/2^-$	1588.2(5)		3(1)	
188.0(4)[a]	222(39)	207(73)	$3/2^-$	1639.3(3)		4(3)	
189.9(3)	9(4)	23(3)	$11/2^+$	2154.9(4)		6(1)	
210.4(5)[†a,b]	329(14)		$5/2^-$	2236.6(5)		7(4)	
326.4(4)[a]	100(41)	114(23)	$7/2^-$	2253.8(4)		8(2)	
365.3(6)[a,b]	37(5)	37(3)	$9/2^-$	2263.5(5)		42(7)	
401.7(3)[b]	117(8)	248(51)	$(5/2^-)$	2265.1(6)[b]			
454.5(1)	63(5)	150(7)	$(5/2^-)$	2311.5(4)[b]		9(3)	
476.3(5)	13(1)	41(3)	$(7/2^-)$	2321.1(5)		29(4)	
532.1(3)	10(2)	36(3)	$(7/2^-)$	2332.0(6)		2(1)	
572.8(8)[a]		19(2)	$(9/2^-)$	2358.8(5)		4(2)	
631.1(4)		5.0(8)	$(9/2^-)$	2375.5(3)[b]		36(5)	
646.4(2)	18(6)	24(2)	$(3/2^+)$	2395.9(4)		66(9)	
669.3(3)	60(3)	87(13)	$(3/2^-)$	2397.1(5)[b]		4(1)	
693.1(3)[a,b]	3.1(8)	8(1)	$(5/2^+)$	2404.5(8)		6(6)	
726.9(3)	41(4)	74(7)	$(5/2^-)$	2411.3(8)		12(3)	
756.9(4)		12(2)	$(7/2^+)$	2440.2(3)		54(4)	
807.0(4)		8(2)		2485.3(5)		208(8)	
807.3(6)[a]		3.2(8)	$(7/2^-)$	2493.0(5)		8(8)	
841.2(3)[a,b]		7(4)	$(9/2^+)$	2516.5(8)		4(3)	
910.1(4)		7(3)	$(9/2^-)$	2528.5(5)[b]		51(3)	
926.0(4)		3.1(5)		2544.3(6)		3.2(7)	
1037.1(3)	58(4)	80(5)		2576.2(7)		4(1)	
1100.7(3)	7(1)	13(3)		2586.5(5)		8(2)	
1307.3(5)		6.0(9)		2662.6(7)		3(2)	
1341.1(4)		11(2)					

[a]These states have observed populating transitions for which the intensity could not be quantified, the reported feeding is a lower limit.
[b]These states have observed depopulating transitions for which the intensity could not be quantified, the reported outflow is a lower limit.

respectively. Similarly, Fig. 3(d) shows coincident spectra for the gate on the 1815.9 keV transition. Therein peaks of 459.1, 481.3, and 531.0 keV correspond to the three transitions from the 669.3 keV level to the 210.4 keV $5/2^-$, 188.0 keV $3/2^-$, and 138.2 keV $1/2^-$ levels, respectively. For both of these coincidence spectra, it is clearly seen that only three transitions are well observed exiting the $3/2^-$ band at each of these levels. Although allowed from a $5/2^-$ level, no transition has been observed to the $7/2^+$ ground-state band from these levels. Similar transitions between the $3/2^-$ band and the $1/2^-$ band in ^{165}Dy are observed. Thus, the 669.3, 726.9, 807.3, and 910.1 keV levels have been tentatively assigned to the $(3/2^-)$ band in ^{163}Gd.

The 454.5 keV level is low enough in energy for anticipated single-particle states and has been tentatively assigned as the $(5/2^-)[512]$ band head along with the 532.1, and 631.1 keV levels as the $(7/2^-)$, and $(9/2^-)$ rotational excitations respectively. The resultant level spacing is consistent with the PSM calculations. It is possible that the 454.5 keV is associated with the $7/2^-[514]$ neutron level resulting in an increase of one spin for all these assignments, both would be consistent with the strong apparent β feeding received by the 454.5 keV level given a $(5/2^-)$ parent ground state.

Evidence for the 171.1 keV transition is weak compared to the other proposed transitions. However, the 171.1 and 74.6 keV transitions would be consistent with the structure of the $5/2^-$ band observed in ^{165}Dy and a (487.4) keV transition has been observed that would be consistent with the placement of a 572.8 keV $9/2^-$ level. The competition between the (487.4) keV transition and the 171.1 keV transition would explain the reduced intensity observed for the 171.1 keV transition. Thus the 171.1 keV transition is not listed as tentative.

The 646.4 keV level observes γ feeding from a number of levels around 2 MeV. Review of the observed γ feeding compared to outflow shows that this level is expected to have no β feeding. As a result, the 646.4 keV level has been tentatively assigned as the band head of the $3/2^+$ band and several similarly low β-fed levels have tentatively been assigned as the rotational excitations at levels 693.1 $(5/2^+)$, 756.9 $(7/2^+)$, and 841.2 $(9/2^+)$ keV.

Table IV lists the internal conversion corrected feeding and outflow observed from γ relative intensity measurements for ^{163}Gd. A review of Table IV shows feeding and outflow relationships consistent with very limited β feedings for both the 85.3 and 189.9 keV levels in the $7/2^+$ ground-state band. The ground state of the parent nucleus is tentatively expected to

have a spin of $5/2^+$ based upon the tentative ground state deformation of the two proton analog of ^{163}Eu, ^{165}Tb. Such a low spin for the ground state of the parent is consistent with the low apparent β feeding of the ground-state band as even the lowest level at 85.3 keV has a spin of $9/2^+$, which would be at least a first forbidden transition. If the parent isotope does indeed have a ground-state spin of $5/2^+$, population of the $3/2^+$ should be preferred to all of the observed bands. A lack of a well-populated $3/2^+$ but strongly populated $1/2^-$, $3/2^-$, and $5/2^-$ bands, offers support of the parent ground state being not $5/2^+$ with deformation similar to the +2 proton neutron analog but $5/2^-$. With a parent ground state of $5/2^-$, the weak population of the even parity bands is reconciled.

Another feature of note observed on Table IV is for the 210.4 keV level, which exhibits an excess of observed γ feeding relative to the observed γ outflow. This is due to the previously discussed unobserved 22.4 keV transition to the 188.0 keV level expected from systematics with ^{165}Dy. This transition is likely present and very strongly internally converted. The existence of this transition would not only help explain the lack of observed transitions from the 210.4 keV level but also the discrepancy between γ feeding and outflow of the 188.0 keV level that otherwise could only be explained by strong direct population of the 188.0 keV level following β decay. Furthermore the 72.2 keV transition was not fit without significant contamination from either background sources or coincident transitions of similar energy, as a result the γ outflow from this level was not ascertained.

A. Potential-energy surface calculations

The configuration-constrained potential-energy surface (PES) method [16] is employed with a nonaxial deformed Woods-Saxon potential [17] with universal parameters to generate single-particle levels. The Lipkin-Nogami method [18] is employed to avoid the spurious transition encountered in the BCS approach. The total energy of a nucleus can be decomposed into a macroscopic part obtained from the standard liquid-drop model and a microscopic part computed with the shell-correction approach including blocking effects. The deformation, excitation energy, and pairing property of a given state are determined by minimizing the obtained PES.

PES calculations were performed for the following configurations: $\nu 1/2^-[521]$, $\nu 7/2^+[633]$, $\nu 5/2^-[523]$, $\nu 5/2^+[642]$, and $\nu 5/2^-[512]$. The deformations yielded by these calculations were consistent with a deformed nucleus without any expected shape coexistence. Figure 4 is the plot of the $\nu 1/2^-[521]$ PES calculation.

B. Projected shell-model calculation

The active nucleon configurations that can be assigned to the bands observed in ^{163}Gd have been calculated using the projected shell model (PSM) [19,20] and those calculated energy levels and comparison with the experimental data are given in Fig. 5. PSM has been successfully applied for studying the structure of isomer states for $A \approx 100$, 160, and 180 neutron-rich mass region [21–23].

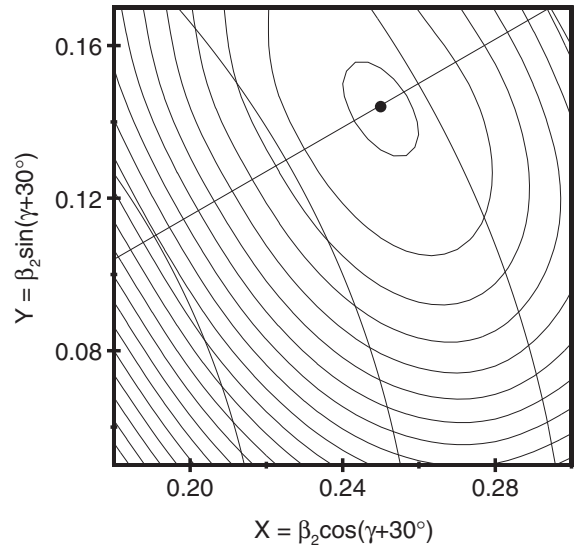

FIG. 4. PES calculation for $\nu 1/2^-[521]$. $\beta_2 = 0.286$, $\gamma = 0$, $\beta_4 = 0.028$.

In the present calculations, we use $\varepsilon_2 = 0.276$, $\varepsilon_4 = 0.000$, a value that is indicated by total Routhian surface calculations [24]. The monopole-pairing strength is taken to be $G_M = [G_1 \mp G_2(N - Z)/A]/A$, "−" for neutrons and "+" for protons, with $G_1 = 20.12$ and $G_2 = 13.13$ being the coupling constants. The quadrupole-pairing strength G_Q is assumed to be proportional to G_M, with the proportionality constant being fixed to be 0.16. These strengths are consistent with those used in previous works for the same mass region [22].

In Fig. 5, rotational bands up to 17/2 of spin are plotted. The dominant configuration for each rotational band is labeled and discussed in the following part below. The calculated $7/2^+[633]$ ground state is in good agreement with the experimental data together with the $N = 99$ systematics [25]. The first excited state is assigned as $1/2^-[521]$ in the PSM calculations, which is in good agreement with the experimental data. The correct placement of the $7/2^+[633]$ and $1/2^-[521]$ neutron single-particle orbital are most important to understand the evidence of the $N = 98$ subshell gap [2,26]. With the neutron Fermi surface moving up, the $5/2^-[523]$ one-quasiparticle (1-qp) state is more excited, which is the ground state for the $N = 97$ isotones in $A \approx 160$ mass region. Both the energy levels and the dominant configuration for these three bands are reproduced well by the PSM calculations. However, the calculated energy levels of the $3/2^-[521]$ 1-qp band are higher than those of experimental data. In Refs. [27,28], β_6 or ε_6 deformation was included in the potential energy surface calculations and cranked shell model, respectively, which is not taken into account in the present calculations. It is expected that theoretical results will be improved with including high order deformation. The predicted energy levels of high spin states in Fig. 5 may provide a guidance to the further experimental work.

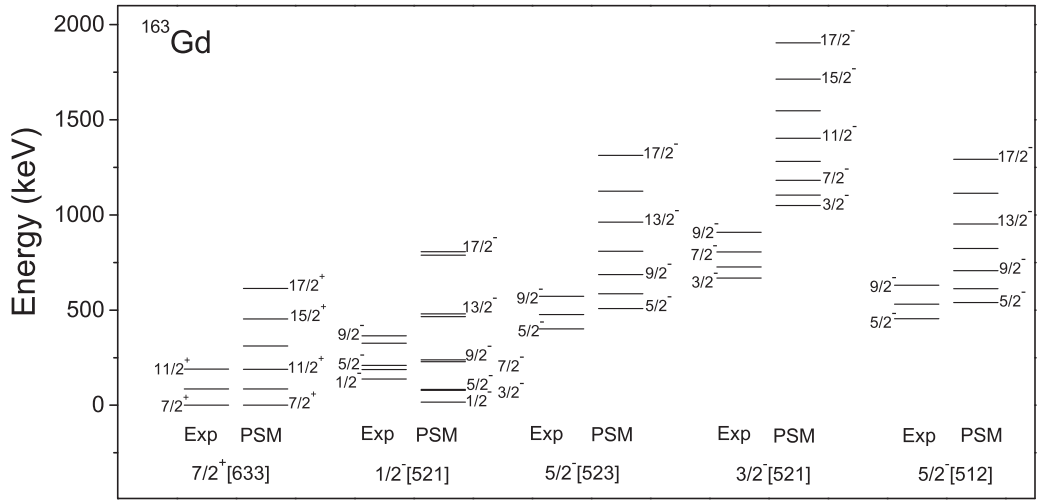

FIG. 5. Comparison of proposed bands of ^{163}Gd with calculated band structure of ^{163}Gd.

V. CONCLUSION

The level structure of ^{163}Gd has been identified for the first time and compared with the structure of ^{165}Dy, the $N = 99$ neutron analog of ^{163}Gd. The level structure includes 107 new γ transitions and 53 new levels. Assignments of the ground-state band and five additional bands have been proposed. The ground state has been assigned a spin of $7/2^+$, commensurate with the ground state of the $+2$ proton neutron-analog ^{165}Dy.

The initial observations of the 137.8 keV level by Hayashi *et al.* [3] as isomeric has been confirmed with the level being observed as the first excited state at 138.2 keV and a spin of $1/2^-$. This assignment is both consistent with the structure of ^{165}Dy and the observation of the level as an isomer. This assignment supports the existence of a subshell gap at $N = 98$ discussed by Hartley *et al.* [2]. Two bands of spin $5/2^-$ are tentatively proposed at 401.7 and 454.5 keV. The 669.3 keV level is tentatively proposed to be the band head of the $3/2^-$ band. Lastly a band head of $3/2^+$ is tentatively proposed at 646.4 keV.

PSM calculations were carried out for a single quadrupole deformation. This is consistent with the PES calculations as they did not yield any expectation of shape coexistence. PSM calculations yielded good agreement with experimentally observed band structures in four out of five cases. For the remaining case of the $3/2^-$ band it is expected that higher-order deformation would need to be included in the calculation to resolve this discrepancy.

Further structure beyond level spacing and observed γ intensities for ^{163}Gd would need to be performed with a setup capable of more complete efficiency, including absolute count of β-decay events and, or, increased angular resolution such that angular correlation measurements could be implemented to make confident spin assignments.

ACKNOWLEDGMENTS

We would like to acknowledge the Holifield Radioactive Ion Beam Facility and staff for their critical role in obtaining these data. Oak Ridge National Laboratory is supported by the U.S. Department of Energy Office of Nuclear Physics. Participants from Vanderbilt University were supported by the U.S. Department of Energy Grant No. DE-FG05-88ER-40407. The U.S. Department of Energy supported participants from Mississippi State University under Grant No. DE-FG02-96ER41006. Participants from the University of Tennessee were funded by the Office of Nuclear Physics, U.S. Department of Energy under Award No. DE-FG02-96ER40983 and the National Nuclear Security Administration under the Stewardship Science Academic Alliances program through DOE Award No. DE-NA0002132. Support for the work done at Huzhou University and Shanghai Jiao Tong University was provided by the National Natural Science Foundation of China Grants No. U1832139, No. 11947410, and No. U1932206, and by the National Key Program for S&T Research and Development Grant No. 2016YFA0400501. Work at Peking University was supported by the National Natural Science Foundation of China Grants No. 11835001 and No. 11921006.

[1] E. F. Jones, J. H. Hamilton, P. M. Gore, A. V. Ramayya, J. K. Hwang, A. P. deLima, S. J. Zhu, Y. X. Luo, C. J. Beyer, J. Kormicki, X. Q. Zhang, W. C. Ma, I. Y. Lee, J. O. Rasmussen, S. C. Wu, T. N. Ginter, P. Fallon, M. Stoyer, J. D. Cole, A. V. Daniel, G. M. Ter-Akopian, R. Donangelo, S. J. Asztalos, T. Cornelius, P. Fleischer, M. Bender, T. Bürvenich, S. Schramm, J. A. Maruhn, and P.-G. Reinhard, J. Phys. G: Nucl. Part. Phys. **30**, L43 (2004).

[2] D. J. Hartley, F. G. Kondev, R. Orford, J. A. Clark, G. Savard, A. D. Ayangeakaa, S. Bottoni, F. Buchinger, M. T. Burkey, M. P. Carpenter, P. Copp, D. A. Gorelov, K. Hicks, C. R. Hoffman, C. Hu, R. V. F. Janssens, J. W. Klimes, T. Lauritsen, J. Sethi, D.

Seweryniak, K. S. Sharma, H. Zhang, S. Zhu, and Y. Zhu, Phys. Rev. Lett. **120**, 182502 (2018).
[3] H. Hayashi, M. Shibata, M. Asai, A. Osa, T. Sato, M. Koizumi, A. Kimura, and M. Oshima, Nucl. Instrum. Methods Phys. Res. A **747**, 41 (2014).
[4] M. Vilen, J. M. Kelly, A. Kankainen, M. Brodeur, A. Aprahamian, L. Canete, T. Eronen, A. Jokinen, T. Kuta, I. D. Moore, M. R. Mumpower, D. A. Nesterenko, H. Penttilä, I. Pohjalainen, W. S. Porter, S. Rinta-Antila, R. Surman, A. Voss, and J. Äystö, Phys. Rev. Lett. **120**, 262701 (2018).
[5] T. K. Sato, A. Osa, K. Tsukada, M. Asai, H. Hayashi, Y. Kojima, M. Shibata, and S. Ichikawa, JAEA-Review **2006-029**, 31 (2006).
[6] R. K. Sheline, W. N. Shelton, H. T. Motz, and R. E. Carter, Phys. Rev. **136**, B351 (1964).
[7] R. C. Greenwood, R. J. Gehrke, J. D. Baker, D. H. Meikrantz, and C. W. Reich, Phys. Rev. C **27**, 1266 (1983).
[8] E. Kaerts, P. H. M. van Assche, S. A. Kerr, F. Hoyler, H. G. Börner, R. F. Casten, and D. D. Warner, Nucl. Phys. A **514**, 173 (1990).
[9] A. Osa, S. ichi Ichikawa, M. Matsuda, T. K. Sato, and S.-C. Jeong, Nucl. Instrum. Methods Phys. Res. B **266**, 4394 (2008).
[10] J. Wu, S. Nishimura, G. Lorusso, P. Möller, E. Ideguchi, P.-H. Regan, G. S. Simpson, P.-A. Söderström, P. M. Walker, H. Watanabe, Z. Y. Xu, H. Baba, F. Browne, R. Daido, P. Doornenbal, Y. F. Fang, N. Fukuda, G. Gey, T. Isobe, Z. Korkulu, P. S. Lee, J. J. Liu, Z. Li, Z. Patel, V. Phong, S. Rice, H. Sakurai, L. Sinclair, T. Sumikama, M. Tanaka, A. Yagi, Y. L. Ye, R. Yokoyama, G. X. Zhang, D. S. Ahn, T. Alharbi, N. Aoi, F. L. Bello Garrote, G. Benzoni, A. M. Bruce, R. J. Carroll, K. Y. Chae, Z. Dombradi, A. Estrade, A. Gottardo, C. J. Griffin, N. Inabe, D. Kameda, H. Kanaoka, I. Kojouharov, F. G. Kondev, T. Kubo, S. Kubono, N. Kurz, I. Kuti, S. Lalkovski, G. J. Lane, E. J. Lee, T. Lokotko, G. Lotay, C.-B. Moon, D. Murai, H. Nishibata, I. Nishizuka, C. R. Nita, A. Odahara, Z. Podolyák, O. J. Roberts, H. Schaffner, C. Shand, Y. Shimizu, H. Suzuki, H. Takeda, J. Taprogge, S. Terashima, Z. Vajta, and S. Yoshida, Phys. Rev. Lett. **118**, 072701 (2017).
[11] R. J. Gehrke, R. C. Greenwood, J. D. Baker, and D. H. Mekrantz, J. Radiol. Nucl. Chem. **74**, 117 (1982).
[12] R. Grzywacz, Nucl. Instrum. Methods Phys. Res. B **204**, 649 (2003).
[13] T. Kibédi, T. Burrows, M. Trzhaskovskaya, P. Davidson, and C. Nestor, Nucl. Instrum. Methods Phys. Res. A **589**, 202 (2008).
[14] H. Nabielek, *Untersuchung von Obergangsraten Elektromagnetischer Ubergange durch Messung der Lebensdauer Angeregter Kernniveaus nach Neutroneneinfang* (Physikinstitut, Reaktorzentrum Seibersdorf, Austria, 1968).
[15] K. Alder and R. M. Steffen, in *The Electromagnetic Interaction in Nuclear Spectroscopy* (North-Holland, Amsterdam, 1975).
[16] F. Xu, P. Walker, J. Sheikh, and R. Wyss, Phys. Lett. B **435**, 257 (1998).
[17] W. Nazarewicz, J. Dudek, R. Bengtsson, T. Bengtsson, and I. Ragnarsson, Nucl. Phys. A **435**, 397 (1985).
[18] H. Pradhan, Y. Nogami, and J. Law, Nucl. Phys. A **201**, 357 (1973).
[19] K. Hara and Y. Sun, Int. J. Mod. Phys. E **4**, 637 (1995).
[20] Y. Sun, Phys. Scr. **91**, 043005 (2016).
[21] Y.-X. Liu, Y. Sun, X.-H. Zhou, Y.-H. Zhang, S.-Y. Yu, Y.-C. Yang, and H. Jin, Nucl. Phys. A **858**, 11 (2011).
[22] Y. C. Yang, Y. Sun, S. J. Zhu, M. Guidry, and C. L. Wu, J. Phys. G: Nucl. Part. Phys. **37**, 085110 (2010).
[23] X.-Y. Wu, S. K. Ghorui, L.-J. Wang, Y. Sun, M. Guidry, and P. M. Walker, Phys. Rev. C **95**, 064314 (2017).
[24] Möller, J. Nix, W. Myers, and W. Swiatecki, At. Data Nucl. Data Tables **59**, 185 (1995).
[25] Z. Patel, P. M. Walker, Z. Podolyák, P. H. Regan, T. A. Berry, P.-A. Söderström, H. Watanabe, E. Ideguchi, G. S. Simpson, S. Nishimura, Q. Wu, F. R. Xu, F. Browne, P. Doornenbal, G. Lorusso, S. Rice, L. Sinclair, T. Sumikama, J. Wu, Z. Y. Xu, N. Aoi, H. Baba, F. L. Bello Garrote, G. Benzoni, R. Daido, Z. Dombrádi, Y. Fang, N. Fukuda, G. Gey, S. Go, A. Gottardo, N. Inabe, T. Isobe, D. Kameda, K. Kobayashi, M. Kobayashi, T. Komatsubara, I. Kojouharov, T. Kubo, N. Kurz, I. Kuti, Z. Li, M. Matsushita, S. Michimasa, C.-B. Moon, H. Nishibata, I. Nishizuka, A. Odahara, E. Şahin, H. Sakurai, H. Schaffner, H. Suzuki, H. Takeda, M. Tanaka, J. Taprogge, Z. Vajta, A. Yagi, and R. Yokoyama, Phys. Rev. C **96**, 034305 (2017).
[26] Y. X. Liu, C. J. Lv, Y. Sun, and F. G. Kondev, J. Phys. G: Nucl. Part. Phys. **47**, 055108 (2020).
[27] Z. Patel, P.-A. Söderström, Z. Podolyák, P. H. Regan, P. M. Walker, H. Watanabe, E. Ideguchi, G. S. Simpson, H. L. Liu, S. Nishimura, Q. Wu, F. R. Xu, F. Browne, P. Doornenbal, G. Lorusso, S. Rice, L. Sinclair, T. Sumikama, J. Wu, Z. Y. Xu, N. Aoi, H. Baba, F. L. Bello Garrote, G. Benzoni, R. Daido, Y. Fang, N. Fukuda, G. Gey, S. Go, A. Gottardo, N. Inabe, T. Isobe, D. Kameda, K. Kobayashi, M. Kobayashi, T. Komatsubara, I. Kojouharov, T. Kubo, N. Kurz, I. Kuti, Z. Li, M. Matsushita, S. Michimasa, C.-B. Moon, H. Nishibata, I. Nishizuka, A. Odahara, E. Şahin, H. Sakurai, H. Schaffner, H. Suzuki, H. Takeda, M. Tanaka, J. Taprogge, Z. Vajta, A. Yagi, and R. Yokoyama, Phys. Rev. Lett. **113**, 262502 (2014).
[28] X.-T. He and Y.-C. Li, Phys. Rev. C **98**, 064314 (2018).